Research Article **Open Access**

B. Divband*, M. R. Rashidi, M. Khatamian, G. R. Kazemi Eslamian, N. Gharehaghaji, F. Dabaghi Tabriz

Linde Type A and nano magnetite/NaA zeolites: cytotoxicity and doxorubicin loading efficiency

https://doi.org/10.1515/chem-2018-0001
received August 16, 2017; accepted October 9, 2017.

Abstract: Different cation-exchanged (K^+, Na^+ & Ca^{2+}) nano-zeolites with magnetite nanocomposites were synthesized and their suitability for drug loading was studied. Nanocomposites with different Fe_3O_4 contents were synthesized by adding magnetic Fe_3O_4 nanoparticles to the zeolite crystallization solution. The zeolite and its nanocomposites had high surface areas and enough adsorption capacity to load and release sufficient amounts of the chemotherapeutic doxorubicin. None of the zeolites or nanocomposites showed toxicity to SKBr3 or MCF-7 cancer cells. However, DOX@zeolite inhibits cell growth more than the non-encapsulated drug. Thus zeolites and their magnetite nanocomposites show potential as biocompatible medical devices.

Keywords: Nano magnetite zeolite, doxorubicin, drug loading capacity, cytocompatibility.

1 Introduction

Biocompatibility, mechanical stability and high drug loading capacity are necessary for drug delivery systems and for slow controlled release. Inorganic carriers have recently been used as drug release systems, but there are few reports of porous matrices as drug carriers [1-4]. Zeolites' low toxicity, high dispersibility, good capacity and surface silanols make them good biomaterials with various applications. They have microporous structures with ordered cages and channels [5,6]. The size and dimensions of the pores, channels and cages, as well as the numbers, sites and types of structural cations affect their drug loading properties [7-12], and drug functional groups can interact with the surface silanols of the zeolites. Zeolites and their composites are used as catalyst supports [13], anticancer drug encapsulants [14-16], antibacterial agents [7,17,18], antihelminthics [19], and anti-inflammatory drugs [20]. Doxorubicin is a cytotoxic and cytostatic drug with a low therapeutic index, used in cancer chemotherapy [21–24]. Zeolites have been reported as slow release carriers [7,24]. For example, zeolite Y is commonly used for encapsulating dichlorvos (2,2-dichlorovinyldimethylphosphate), ibuprofen (anti-inflammatory) [25], 5-fluorouracil [26], erythromycin, carbamazepine, levofloxacin [27], and aspirin (acetylsalicylic acid) [28]. Clinoptilolite is a natural zeolite used to carry erythromycin in topical acne therapy [19], aspirin [29], and sulfamethoxazole [30]. Zeolite A is an important molecular sieve due to its high adsorption and easy sodium exchange for cations (calcium, potassium, iron, *etc*). [31,32]. There have been few studies of zeolite A as a drug carrier [33,34].

Magnetic drug targeting using magnetite core-shell composites to achieve biocompatiblity and porosity for drug adsorption or encapsulation is an emerging improvement over conventional cancer treatment methods. A magnetic field is applied to direct the composite to the tumor proximity. This can significantly reduce the necessary dose and minimize side effects [35].

Magnetite-zeolites may prove effective drug delivery composites because of the zeolite properties as well as preventing magnetite agglomeration. There has been only one report; magnetite-FAU zeolite was prepared by mechanical activation but no toxicity results were reported [34,35]. A novel magnetic zeolite as a potential MR imaging agent has been recently reported [36].

The purpose of the present work was to examine the nano-zeolites (KA, NaA, CaA) and nano-magnetite zeolite (Fe_3O_4/NaA) as *in vitro* magnetite drug delivery systems for the anticancer drug doxorubicin (DOX), on two different breast cell lines, SKBR3 and SCF7.

***Corresponding author: B. Divband:** Research Center for Pharmaceutical Nanotechnology, Tabriz University of Medical Sciences, Tabriz, Iran; Inorganic Chemistry Department, Faculty of Chemistry, University of Tabriz, C.P. 51664, Tabriz, Iran, E-mail: divband@tabrizu.ac.ir
M. R. Rashidi: Research Center for Pharmaceutical Nanotechnology, Tabriz University of Medical Sciences, Tabriz, Iran; Faculty of Pharmacy, Tabriz University of Medical Sciences, Tabriz, Iran
M. Khatamian: Inorganic Chemistry Department, Faculty of Chemistry, University of Tabriz, C.P. 51664, Tabriz, Iran
G. R. Kazemi Eslamian, N. Gharehaghaji: Radiology Department, Faculty of Paramedicine, Tabriz University of Medical Sciences, Tabriz, Iran
F. Dabaghi: Operative Dentistry Department, Faculty of Dentistry, Tabriz University of Medical Sciences, Tabriz, Iran

2 Methods

2.1 Materials

Ferrous chloride ($FeCl_2 \cdot 4H_2O$), ferric chloride hexahydrate ($FeCl_3 \cdot 6H_2O$), sodium aluminate, sodium hydroxide, $CaCl_2$, and KCl were purchased from Merck and local clinoptilolite was used. SKBR3 and SCF7 human breast cancer cell lines were purchased from the National Cell Bank of Iran, Pasteur Institute of Iran, Tehran, Iran. MTT (3-(4,5-dimethylthiazol-2-yl)-2,5-diphenyl- tetrazolium bromide) and Cell Death Detection ELISAPLUS kit were purchased from Roche Diagnostics GmbH, Mannheim, Germany.

2.2 Synthesis of nano-zeolites

Nano-zeolite NaA was synthesized hydrothermally from annealed local clinoptilolite after crushing, drying, screening and washing. Clinoptilolite, sodium hydroxide, sodium aluminate and distilled water were mixed for 6h (aging). The resulting gel was treated by ultrasound for 6h, transferred to a Teflon-lined stainless steel autoclave, and heated at autogenous pressure in an air oven at 353 K. After a suitable time (the pH reached 7) the suspension was centrifuged several times and the product was dried. For the preparation of CaA (5A) and KA (6A) nano-zeolites, calcium and potassium hydroxide replaced the sodium hydroxide. The products were characterized and their adsorption properties examined.

For synthesis of nano-magnetic NaA, magnetic Fe_3O_4 was synthesized by co-precipitation from an alkaline solution of Fe^{2+} and Fe^{3+} salts and added to the carrier gel [37] after the ultrasound treatment. The next steps were same as the synthesis of nano-zeolite NaA. Nano-magnetite NaA with different Fe_3O_4 loadings (0, 2.1, 4 and 7.7 wt.%) was prepared by varying the amount of nano-Fe_3O_4 and designated as M_n4A (n=0, 2.1, 4 & 7.7).

2.3 Doxorubicin standard solutions preparation

Standard solutions of doxorubicin (5, 50, 100 mgL^{-1}) in deionized water were prepared quickly and kept in the dark because light immediately changes doxorubicin to a toxic material.

2.4 Preparation of drug loaded nano-zeolites

20 mg of each nano-zeolite was added to 20 mL of the standard doxorubicin solutions and stirred for 24 hours at room temperature. The white zeolite changed to the red doxorubicin color as the drug entered the zeolite pores and the loading was complete. Doxorubicin disappearance was confirmed by supernatant absorbance measurement with a Shimadzu UV-240 spectrophotometer at 485 nm. After there were no further changes in the liquid phase concentration it was assumed that the loading capacity had been reached. The reddish solid was separated by filtration, air-dried for 24h and designated DOX_n@ZA (n= 0, 5, 50, 100 & 500).

Desorption was examined at 37ºC, but the loaded nanocomposite was first washed and dried to remove non-adsorbed doxorubicin. The release profile was obtained by dispersing 100 mg of dried drug-loaded nano-zeolite in 50 mL of buffer (pH= 7.4, 5.5). As in the uptake experiments, the concentration of doxorubicin in the particle-free liquid was determined at fixed time intervals.

2.5 Measurements

A Siemens D500 diffractometer with Cu Kα radiation (λ=1.5418 Å and θ=4-80°) was used to characterize the powders. Functional group absorption bands were studied with a Bruker Tensor 27 FTIR as KBr pellets. Gold-coated particle morphology, size and elemental composition were analyzed with a Philips XL30 SEM. SEM was done at 5Kv while EDX analysis was at 15Kv.The BET surface area was measured by N_2 adsorption–desorption isotherms at liquid nitrogen temperature a using NOVA2000 (Quantachrome, USA). TEM and EDX of the samples were performed on a Zeiss LEO 912 Omega at 120 kV. TEM specimens were made by evaporating one drop of ethanolic solution on carbon-coated copper grids and blotted dry on filter paper. Magnetic properties were investigated at room temperature using a 7400 vibrating sample magnetometer.

2.6 MTT assay

The effects of concentrations of the carrier, drug and drug-loaded carrier on cell viability were investigated using identical methods.

SKBR3 and SCF7 cell lines were grown in sterile RPMI-1640 media containing 10% fetal bovine serum, streptomycin (100 μg/mL), amphotericin B (0.25 μg/mL) and penicillin (100 U/mL) at 5% CO_2 in a humidified 37°C

incubator. Then 200 µL/well of supplemented medium and 12×10^3 cells were incubated in 96-well plates for 24 hours at 37°C and 5% CO_2. The cells were divided into four groups in triplicate: blank, drug, carrier and drug-loaded carrier supplemented.

A Cell Death Detection ELISAPLUS kit was used according to the manufacturer's protocol to induce cell apoptosis and necrosis. Briefly, supernatants and cell lysates were prepared and incubated in microtiter plates coated with an antihistone antibody then analyzed at 405 nm.

After incubation the used media were discarded and the wells washed with pH 7.4 phosphate-buffered saline. 50 µL of 2 mg/mL MTT solution and 150 µL culture medium were added to each well. The cells were incubated at 37°C and 5% CO_2 for 24 hours; then the media was removed and 200 µL of dimethyl sulfoxide and 25µL Sorenson solubilizer buffer added to each well. Finally, an ELISA plate reader (BioTeck, Bad Friedrichshall, Germany) was used to read the absorbance at 405 nm. All results were analyzed relative to the untreated cells then normalized.

Ethical approval: The conducted research is not related to either human or animals use.

3 Results

3.1 Characterization of DOX@ZA

Figure 1A shows the pXRD of zeolite 4A before and after DOX loading. All characteristic peaks of zeolite 4A are shown. In Figures 1A(b-d), 4.7ppm, 42.5ppm and 80ppm DOX were loaded. XRD pattern similarity before and after drug loading indicates that the framework did not change. However, overall reduction in the peaks' intensity indicated a slight decrease in zeolite crystallinity following drug adsorption which is more obvious at higher drug loadings. The XRD patterns of the other zeolites are similar.

The XRD show only characteristic 4A zeolite and Fe_3O_4 peaks; no other structures or changes in cell parameters were observed (Figure 1B). The XRD of the $DOX_n@M_4$4A (n = 42.5ppm and 80ppm; Figures 1B (a-c)) were similar to the $M_4$4A XRD with reduced peak intensities.

TEM and SEM examined nano-zeolite morphology before and after loading. The DOX@ZA with the lowest DOX concentration (5 ppm) is shown in Figure 2a. The morphology and structure were unchanged after drug loading. As DOX is larger than the nano-zeolite pores, it is

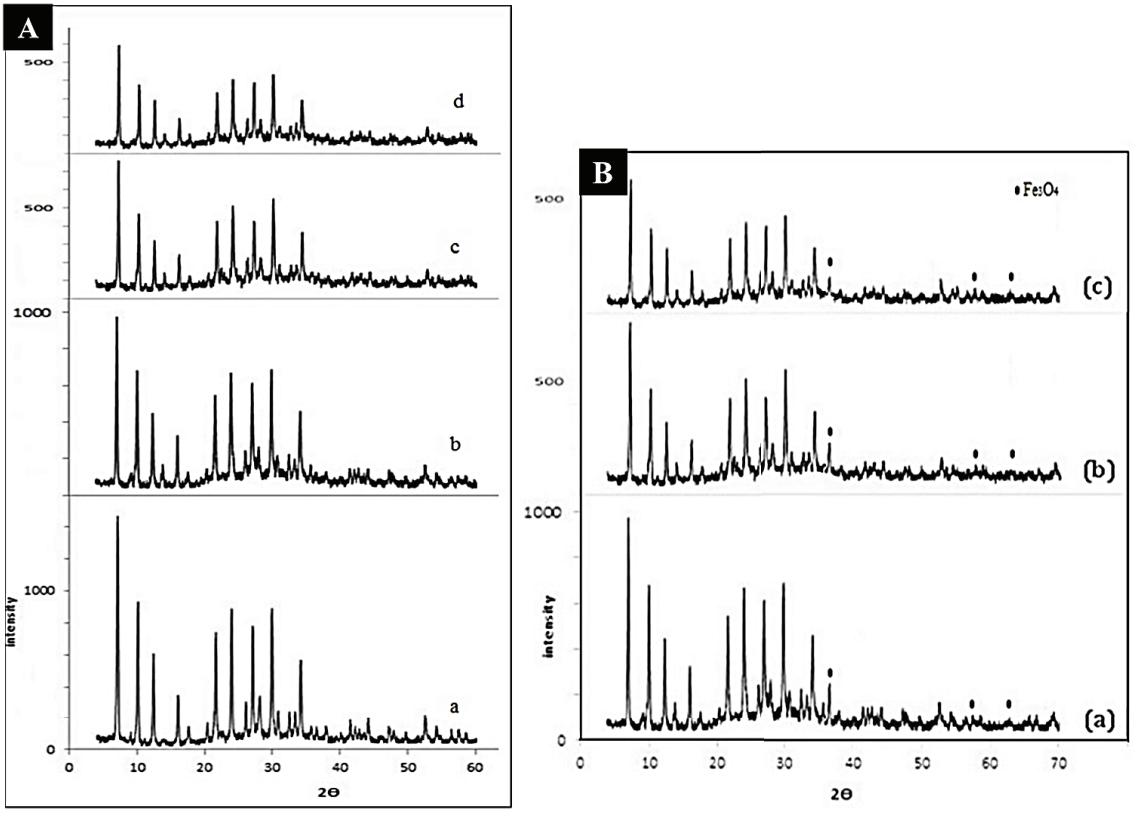

Figure 1: XRD patterns of: A) a: zeolite 4A, b: $DOX_{4.7}$ @ 4A, c: $DOX_{42.5}$ @ 4A, d: DOX_{80} @ 4A; B) a: $M_4$4A, b: $DOX_{42.5}$ @ $M_4$4A, c: DOX_{80} @$M_4$4A.

adsorbed on the outer surface. Drug and zeolite -OH and $-NH_2$ groups hydrogen bond causing aggregation. The average particle size of the starting 4A was about 50-100 nm (Figure 2b) and 80-120 nm for M4A (Figure 3a).

3.2 Loading efficiency and release

4A zeolite (94% of DOX_5@ZA) has significantly higher loading efficiency than 3A and 5A zeolites (86% and 79%) as shown in Figure 4a. The higher amounts of DOX in the 4A zeolite suggest higher drug loadings in the pores due to different pore sizes. The initial red of the DOX solution became colorless after a few minutes of zeolites contact; respectively, 92%, 84% and 74% of the initial DOX was adsorbed in 30 min by 4A, 3A and 5A (Figure 4a). Adsorption of the remaining DOX was slower and saturation was complete in approximately 120 min. DOX solution UV spectral changes after contact with zeolites were not significant, indicating that their interaction is only physical.

Hydrogen bonding of the DOX $-NH_2(\delta^+)$ groups to the zeolite $-OH$ (δ^-) groups causes drug loading.

$$\text{Loading efficiency } (\%) = \frac{DOX\ in\ zeolite - free\ DOX}{DOX\ in\ zeolite} \times 100\%$$

At higher DOX concentrations (DOX_{50}@ZA and DOX_{100}@ZA), loading efficiency was lower (Figure 4b). The mean pore size of the A zeolites is 0.87 nm which is much smaller than the DOX molecule, so adsorption occurred only on the external surface as a poremouth phenomenon [34]. The 4A BET external specific surface area of 5.27 m^2/g means that although the nanocomposite has a considerable DOX storage capacity, the composite surface area (≈ 220-255 m^2g^{-1}) will not be fully occupied. Its loading may come from physical attachment rather than encapsulation.. Substrate surface electronic structure and charge transfer dynamics can strongly influence interactions with the adsorbate.

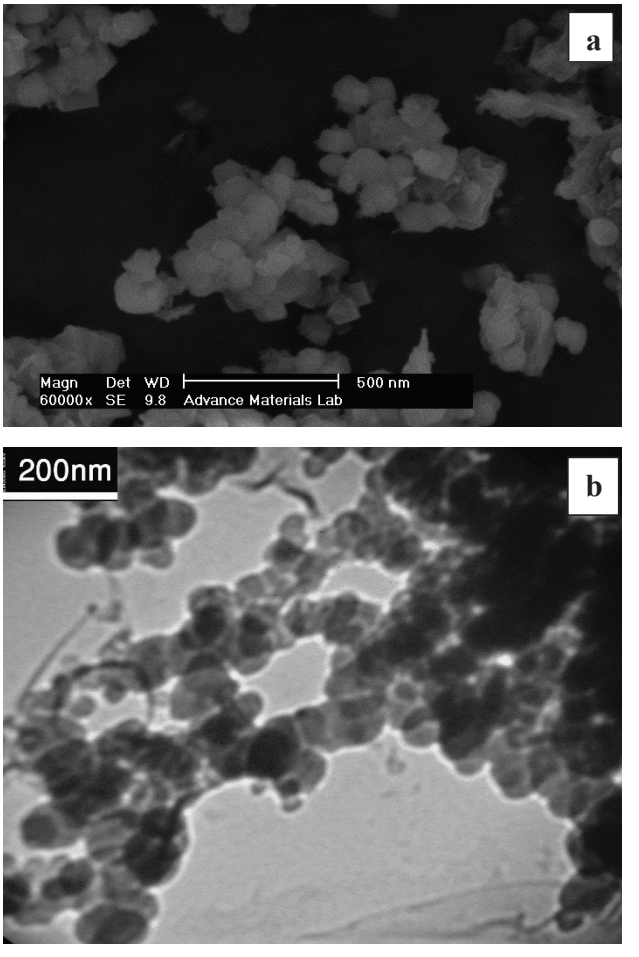

Figure 2: SEM images of: a) DOX_5@ 4A, b) TEM image of 4A.

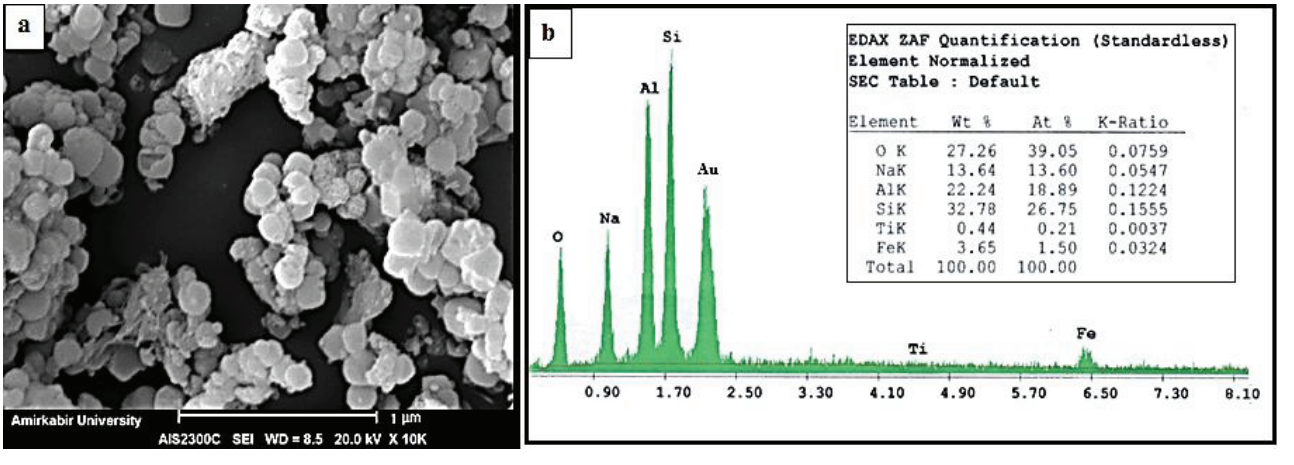

Figure 3: a)SEM image of $M_4$4A, b) EDX of $M_4$4A.

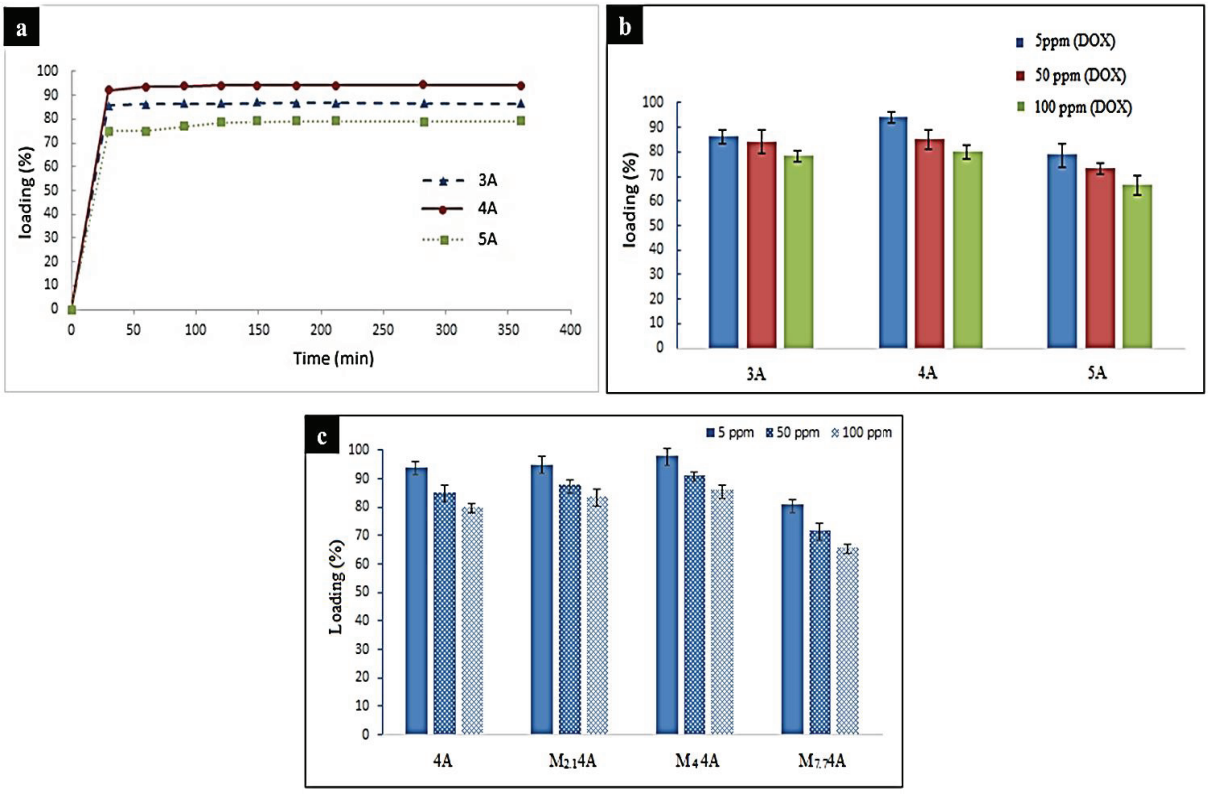

Figure 4: Drug loading efficiency of a) 3A, 4A &5A; b) A type zeolites with different amounts of DOX; c) 4A and M_n4A for different amounts of DOX.

The DOX concentration in DOX_5@ZA is very low; after 24 h approximately 60% of the loaded drug (4.7 ppm from 5 ppm) was released.

Initial DOX uptake by magnetite–zeolite nanocomposites (M4A) was very fast, with 94% adsorption in 30 min. Drug saturation was completed in approximately 2 h. At higher DOX concentrations drug loading was lower for all the composites (Figure 4c). As shown in Figure 4, drug loading increased with increased Fe_3O_4 percentage but at the highest percentage (7.7%) the loading decreased. At 4 wt% Fe_3O_4, maximum adsorption was achieved because the iron oxide was well dispersed into the zeolite pores, caused by strong interactions between the zeolite oxygen atoms and Fe_3O_4. Increasing the Fe_3O_4 content blocked the channels, reducing adsorption.

The dried nanocomposite contains more than 75% drug. Its release was measured by desorption and diffusion into pH 7.4 buffer; released DOX % is given by:

$$Drug\ release\ (\%) = \frac{DOX\ released\ at\ specified\ time}{DOX\ loaded}$$

22% (9.24 ppm), 26% (11.06 ppm), 22% (9.02 ppm) and 21% (9.55 ppm) of the DOX on the 3A, 4A, 5A zeolites and $M_4$4A nanocomposite was released in 24 h. However, at the lower cancer cell pH (5.4), more desorption from DOX_{50}@ZA occurred (70-80%). The release profiles of DOX_5@ZA are the same. There was no dependence of the (DOX@ZA) characteristics on the storage time.

Arruebo *et.al* reported magnetite/Y zeolite prepared by milling as a potential DOX delivery vehicle. They found 92% of DOX adsorbed in 25 h and 77% of the load was released in 12.6 h [34].

3.3 Cytotoxicity of the combination of nano-zeolite with doxorubicin

For breast cancer, the required DOX dosage is 50 mg/m^2 times the Mosteller value for the BSA (body surface area) [38]:

$$BSA\ (m^2) = [Height\ (cm) \times Weight\ (kg)/3600]^{1/2}$$

For a 170 cm, 65 kg female the required DOX dosage is 87.7 mg. Her total body water (TBW) is calculated by Watson's formula [39]:

$$Female\ TBW = (-2.097) + [0.1069 + height\ (cm)] + [0.2466 \times weight\ (kg)]$$

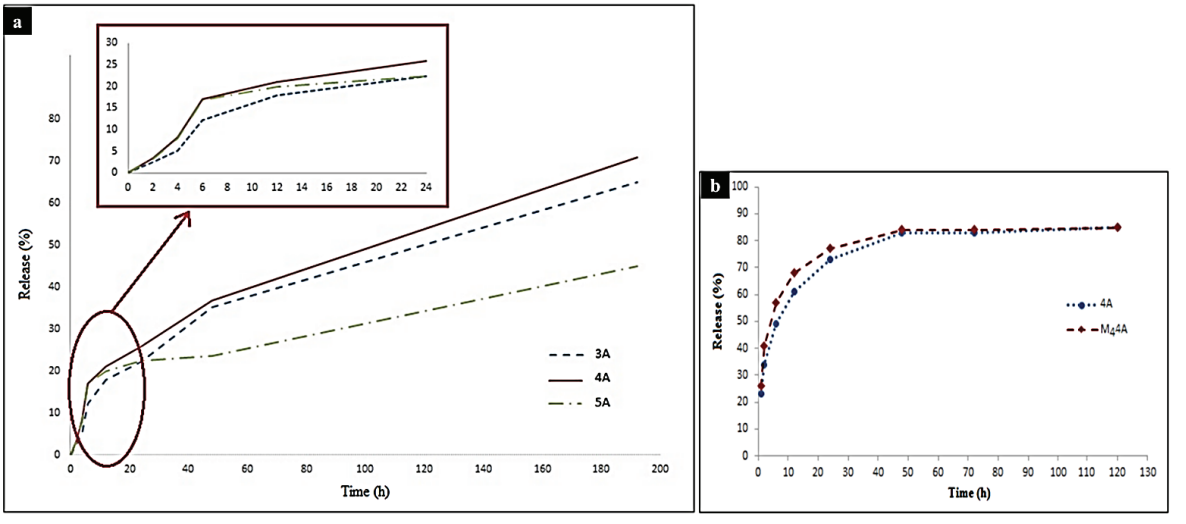

Figure 5: Release profiles of a) DOX_{50} @ ZA (3A, 4A, 5A); b) DOX_{50} @ 4A and DOX_{50} @ $M_4$4A .

Therefore, the DOX concentration should be 2.73 μg/mL. Based on the DOX = 5 ppm loading and release profiles, we achieve this concentration in 25 min from 4A and 20 min from $M_4$4A, respectively. DOX@ZA was selected for the rest of the study.

Zeolites should have small or no effect on cell viability to achieve a suitable delivery system. Investigation of the starting zeolites' cytotoxicity was carried out with the SKBr3 & MCF-7 cell lines. Different DOX_5@ZA concentrations (0.50, 1.00, 2.50 and 5.00 mg/mL) were suspended in the culture medium (RPMI 1640) and treated with ultrasound for 2 min before use for better homogeneity.

Figure 6 illustrates the effect of increasing carrier amounts (zeolites and composites) on cell viability determined by the MTT assay ($P > 0.05$). The insignificant differences between controls (no zeolite) and zeolite concentrations tested show that 3A, 4A & 5A zeolites are not cytotoxic over the 24h incubation period. All of the zeolites and composites gave similar results for a 48 h incubation. For magnetite zeolites containing 7.7% Fe_3O_4 cell viability decreased, but very mild toxicities appeared. $M_4$4A magnetic nanocomposites had no cytotoxicity suggesting biomedical application.

The effects of DOX_5@ZA concentration and zeolite type (3A, 4A, 5A & $M_{3,4}$4A) on SKBr3 & MCF-7 cell viability were investigated. When the DOX_5@ZA concentrations (0.5, 1.0, and 2.5 mg/mL) increased, cell growth inhibition was observed in both cancer cell lines (Figure7). Loading doxorubicin on zeolite improves tumor inhibition over doxorubicin alone.

This increased efficacy may be due to slow release. We believe that like other systems [33,40-42], zeolite delivery systems increase the bioavailability and promote DOX entry into the cell, explaining this increase in potency. Upon exposure to the acidic endosomes/lysosomes environment, DOX is released intracellularly, resulting in efficient apoptotic cell death [43]. Figure 7 shows the treatment-induced apoptosis (> 80%) and necrosis (< 20%), obtained from ELISA analysis for the SKBR3 line.

As shown in Figure 8, the cytotoxicity of delivery with type A zeolite (1.0 mg/mL) was more pronounced for 4A and $M_4$4A, which have greatest loading and release capacity.

Figure 9 shows the $M_4$4A magnetization curve at room temperature. The nanocomposite showed superparamagnetism and the curve's coercivity was negligible. The saturation magnetization and susceptibility values for the nanocomposite were found to be 43.4 emu/gFe and 17.65 emu/gFe kOe, respectively.

4 Conclusion

Linde type A zeolites and their magnetite nanocomposites can be used for efficient loading and slow release applications. Parent zeolites and their nanocomposites were nontoxic to SKBr3 and MCF-7 cells. DOX@4A and DOX@M4A had higher tumor inhibition efficiency compared to other DOX@zeolites and doxorubicin alone.

Acknowledgement: This work was financially supported by the Iran National Science Foundation: INSF (Grant No. 92012004).

Conflict of interest: The authors state no conflict of interest.

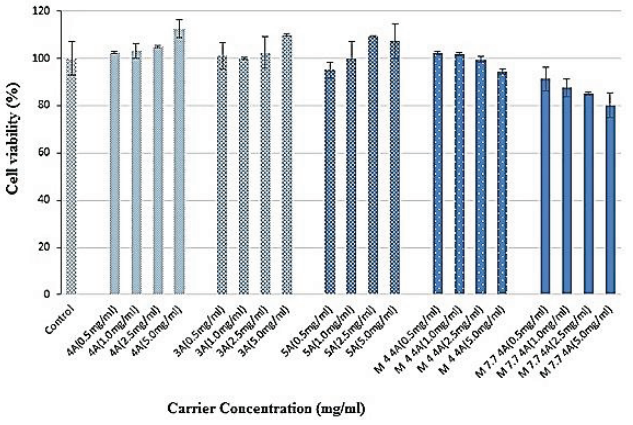

Figure 6: Effect of the different starting zeolites and magnetite form on the SKBr3 cell viability.

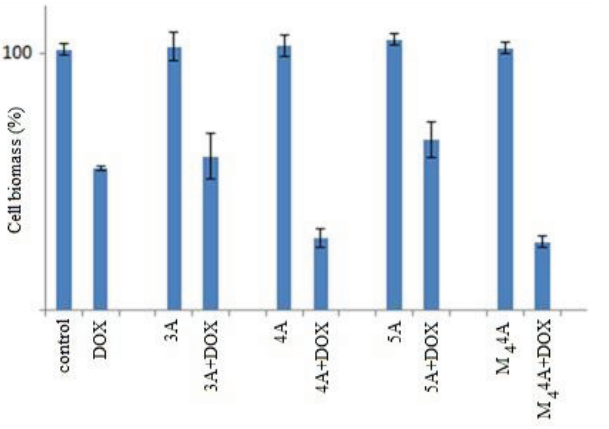

Figure 8: Effect of 1.0 mg/mL of DOX and DOX@ZA (3A, 4A, 5A &$M_4$4A) on the SKBr3 cell viability.

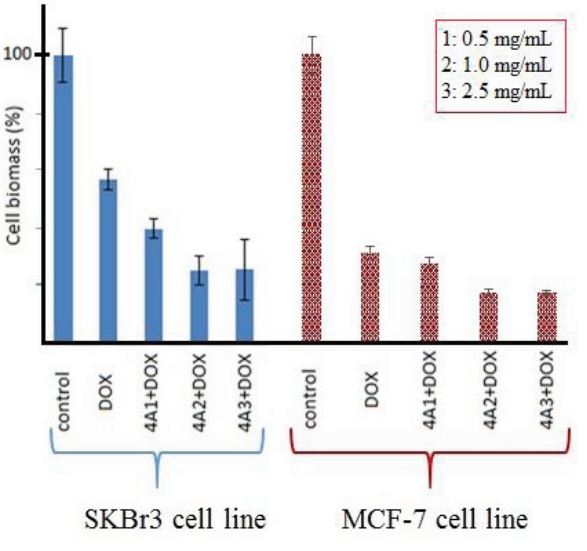

Figure 7: effect of DOX and DOX@4A on the SKBr3 and MCF-7 cells viability.

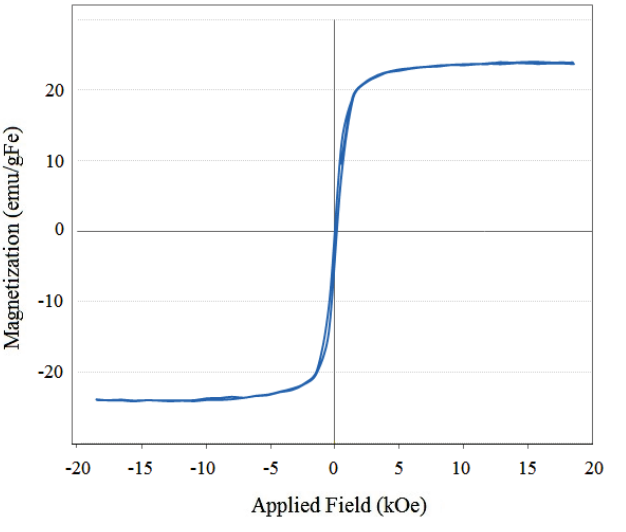

Figure 9: Magnetization versus applied field curve of $M_4$4A nanocomposites.

References

[1] Tang Q., Xu Y., Wu D., Sun Y., Wang J., Xu J., Deng F., Studies on a new carrier of trimethylsilyl-modified mesoporous material for controlled drug delivery. J. Controlled Release 2006, 114, 41–46.

[2] Jämstorp E., Forsgren J., Bredenberg S., Engqvist H., Strømme M., Mechanically strong geopolymers offer new possibilities in treatment of chronic pain. J. Controlled Release, 2010, 146, 370-377.

[3] Verraedt E., Pendela M., Adams E., Hoogmartens J., Martens J.A., Controlled release of chlorhexidine from amorphous microporous silica. J. Controlled Release, 2010, 142, 47-52

[4] Rimoli M.G., Rabaioli M.R., Melisi D., Curcio A., Mondello S., Mirabelli R., Abignente E., Synthetic zeolites as a new tool for drug delivery. J. Biomed. Mater. Res. A., 2008, 87(1), 156-164.

[5] Baerlocher S., McCusker L.B., Olsen DH. Atlas of zeolite framework types. 6th ed. Amsterdam: Elsevier Science, 2007.

[6] Cundy C.S., Cox P.A., The hydrothermal synthesis of zeolites: history and development from the earliest days to the present time. Chem. Rev., 2003, 103, 663-702.

[7] Dyer A., Morgan S., Wells P., Williams C., The use of zeolites as slow release anthelmintic carriers. J. Helminthol., 2000, 74, 137-41.

[8] Horcajada P., Marquez-Alvarez C., Ramila A., Perez-Pariente J., Vallet- Regi M., Controlled release of ibuprofen from dealuminated faujasites. Solid State Sci., 2006, 8, 1459-65.

[9] Grund S., Doussineau T., Fischer D., Mohr G.J., Mitoxantrone-loaded zeolite beta nanoparticles: preparation, physico-chemical characterization and biological evaluation. J. Colloid Interface Sci., 2012, 365, 33-40.

[10] Datt A., Fields D., Larsen S.C., An experimental and computational study of the loading and release of aspirin from zeolite HY. J. Phys. Chem. C., 2012, 116, 21382-90.

[11] Fatouros D.G., Douroumis D., Nikolakis V., Ntais S., Moschovi A.M., Trivedi V., et al., In vitro and in silico investigations of drug delivery via zeolite BEA. J. Mater. Chem., 2011, 21, 7789-94.

[12] Rivera A., Farias T., Ruiz-Salvador A.R., de Menorval L.C., Preliminary characterization of drug support systems based on natural clinoptilolite, Microporous and Mesoporous Materials, 2003, 61, 249–259.

[13] Khatamian M., Divband B., Jodaei A., Degradation of 4-nitrophenol (4-NP) using ZnO nanoparticles supported on zeolites and modeling of experimental results by artificial neural networks. Materials Chemistry and Physics, 2012, 134, 31-37.

[14] Spanakis M., Bouropoulos N., et al., Controlled release of 5-fluorouracil from microporous zeolites, Nanomedicine: Nanotechnology, Biology, and Medicine, 2014, 10, 197–205

[15] Khatamian M., Divband B., Farahmand-Zahed F., Synthesis and characterization of Zinc (II)-loaded Zeolite/Graphene oxide nanocomposite as a new drug carrier, Mater. Sci. Eng. C., 2016, 66, 251–258.

[16] Akalin E., Akyuz S., Akyuz T., Adsorption and interaction of 5-Xuorouracil with montmorillonite and saponite by FT-IR spectroscopy, Journal of Molecular Structure, 2007, 834–836, 477–481.

[17] Ninan N., Thomas S., Grohens Y., Zeolites incorporated polymeric gel beads-Promising drug carriers, Materials Letters, 2014, 118, 12–16

[18] Fox S., Wilkinson T.S., Wheatley P.S., Xiao B., Morris R.E., Sutherland A., et al., NO-loaded $Zn^{(2+)}$-exchanged zeolite materials: a potential bifunctional anti-bacterial strategy. Acta Biomater., 2010, 6, 1515–21.

[19] Cerri G., de Gennaro M., Bonferoni M.C., Caramella C., Zeolites in biomedical application: Zn-exchanged clinoptilolite-rich rock as active carrier for antibiotics in anti-acne topical therapy Appl. Clay Sci., 2004, 27, 141.

[20] Climent M.J., Corma A., Iborra S., Synthesis of nonsteroidal drugs with anti-inflammatory and analgesic activities with zeolites and mesoporous molecular sieve catalysts. J. Catal., 2005, 233, 308–16.

[21] Yoo H.S., Park T.G., Biodegradable polymeric micelles composed of doxorubicin conjugated PLGA-PEG block copolymer. J. Controlled Release, 2001, 70, 63.

[22] Fan H., Dash A.K., Effect of Cross-linking on the In Vitro Release Kinetics of Doxorubicin From Gelatin Implants. Int. J. Pharm., 2001, 213, 103.

[23] Domb A., Davidson G.W., Sanders L.M., Diffusion of peptides through hydrogel membranes. J. Controlled Release, 1990, 14, 133.

[24] Deng B.Y., Deng C., Qi D., Liu C., Liu J., Zhang X., Zhao D., Synthesis of core/shell colloidal magnetic zeolite microspheres for the immobilization of trypsin, Adv. Mater., 2009, 21, 1377–1382.

[25] Horcajada P., Márquez-Alvarez C., Rámila A., Pérez-Pariente J., Vallet-Regí M., Controlled release of Ibuprofen from dealuminated faujasites. Solid State Sciences, 2006, 8, 1459–1465.

[26] Datt A., Burns E.A., Dhuna N.A., Larsen S.C., Loading and release of 5-fluorouracil from HY zeolites with varying SiO_2/Al_2O_3 ratios. Micropor. Mesopor. Mater., 2013, 167, 182–187.

[27] Martucci A., Pasti L., Marchetti N., Cavazzini A., Dondi F., Alberti A., Adsorption of pharmaceuticals from aqueous solutions on synthetic zeolites, Micropor. Mesopor. Mater., 2012, 148, 174–183.

[28] Datt A., Fields D., Larsen S.C., An Experimental and Computational Study of the Loading and Release of Aspirin from Zeolite HY, J. Phys. Chem. C., 2012, 116, 21382–21390

[29] Rivera A., Rodríguez-Albelo L.M., Rodríguez-Fuentes G., Altshuler E., Interaction studies between aspirin and purified natural clinoptilolite, Stud. Surf. Sci. Catal., 2001, 135, 373.

[30] Rivera A., Farías T., Clinoptilolite–surfactant composites as drug support: A new potential application. Micropor. Mesopor. Mater., 2005, 80, 337.

[31] Breck D.W., Zeolite Molecular Sieves: Structure, Chemistry and Uses, John Wiley & Sons, New York, 1974, p. 771.

[32] Barrer R.M., Hydrothermal Chemistry of Zeolites, Academic Press, London, 1982, p. 360.

[33] Amorim R., Vilaça N., Martinho O., Reis R.M., Sardo M., Rocha J., Fonseca A.M., Baltazar F., Neves I.C., Zeolite Structures Loading with an Anticancer Compound As Drug Delivery Systems, J. Phys. Chem. C, 2012, 116, 25642–25650.

[34] Arruebo M., Fernandez-Pacheco R., Irusta S., Arbiol J., Ibarra M.R., Santamar J., Sustained release of doxorubicin from zeolite–magnetite nanocomposites prepared by mechanical activation, Nanotechnology, 2006, 17, 4057–4064.

[35] Neuberger T., Schopf B., Hofmann H., Hofmann M., Rechenberg B. von, Superparamagnetic nanoparticles for biomedical applications: Possibilities and limitations of a new drug delivery system, J. Magn. Magn. Mater., 2005, 293, 483-496.

[36] Atashi Z., Divband B., Keshtkar A., Khatamian M., Farahmand-Zahed F., Kiani Nazarlo A., Gharehaghaji N., Synthesis of cytocompatible Fe_3O_4@ZSM-5 nanocomposite as magnetic resonance imaging contrast agent, J. Magn. Magn. Mater., 2017, 438, 46–51.

[37] Hong R.Y., Zhang S.Z., Han Y.P., Li H.Z., Ding J., Zheng Y., Preparation, characterization and application of bilayer surfactant-stabilized ferrofluids, Powder Technology, 2006, 170, 1–11.

[38] Mosteller R.D., Simplified Calculation of Body Surface Area. N. Engl. J. Med., 1987, 317(17), 1098.

[39] Watson P.E., Watson I.D., Batt R.D. ,Total body water volumes for adult males and females estimated from simple anthropometric measurements. Am. J. Clin. Nutr., 1980, 33, 27-39.

[40] Anglin E.J., Cheng L., Freeman Q.R., Sailor M.J., Porous silicon in drug delivery devices and materials. Adv. Drug Deliver Rev., 2008, 60, 1266–1277.

[41] Vivero-Escoto J.L., Slowing I.I., Trewyn B.G., Lin V.S.-Y., Mesoporous Silica Nanoparticles for Intracellular Controlled Drug Delivery, Small, 2010, 6(18), 1952–1967.

[42] Zhu Y., Ikoma T., Hanagata N., Kaskel S., Rattle-Type Fe_3O_4@ SiO_2 Hollow Mesoporous Spheres as Carriers for Drug Delivery, Small, 2010, 6(3), 471–478.

[43] Aghaee F., Pirayesh Islamian J., Baradaran B., Mesbahi A., Mohammadzadeh M., Asghari Jafarabadi M., Enhancing the Effects of Low Dose Doxorubicin Treatment by the Radiation in T47D and SKBR3 Breast Cancer Cells. J. Breast Cancer, 2013, 16(2), 164-170.